

Provided for non-commercial research and education use.
Not for reproduction, distribution or commercial use.



This article appeared in a journal published by Elsevier. The attached copy is furnished to the author for internal non-commercial research and education use, including for instruction at the authors institution and sharing with colleagues.

Other uses, including reproduction and distribution, or selling or licensing copies, or posting to personal, institutional or third party websites are prohibited.

In most cases authors are permitted to post their version of the article (e.g. in Word or Tex form) to their personal website or institutional repository. Authors requiring further information regarding Elsevier's archiving and manuscript policies are encouraged to visit:

<http://www.elsevier.com/copyright>



Nitrogen-doping effects on the growth, structure and electrical performance of carbon nanotubes obtained by spray pyrolysis method

Mihnea Ioan Ionescu^a, Yong Zhang^a, Ruying Li^a, Hakima Abou-Rachid^b, Xueliang Sun^{a,*}

^a Department of Mechanical and Materials Engineering, University of Western Ontario, London, ON N6A 5B9, Canada

^b Defense Research & Development Canada – Valcartier, 2459 Boulevard PieXI Nord, Québec, QC G3J 1X5, Canada

ARTICLE INFO

Article history:

Received 6 June 2011

Received in revised form

16 November 2011

Accepted 5 January 2012

Available online 12 January 2012

Keywords:

Carbon nanotubes

Chemical vapor deposition

Spray pyrolysis

ABSTRACT

Vertically aligned nitrogen-doped carbon nanotubes (CNTs) with modulated nitrogen content have been synthesized in a large scale by using spray pyrolysis chemical vapor deposition technique. The effects of nitrogen doping on the growth, structure and electrical performance of carbon nanotubes have been systematically examined. Field emission scanning electron microscopy, transmission electron microscopy, X-ray photoelectron spectroscopy, and Raman techniques have been employed to characterize the morphology, composition, and vibrational properties of nanotubes. The results indicate that the nitrogen incorporation significantly influences the growth rate, morphology, size and structure of nanotubes. Electrical measurement investigation of the nanotubes indicates that the change in electrical resistance increases with temperature and pressure as the nitrogen concentration increases inside the tubes. This work presents a versatile, safe, and easy way to scale up route of growing carbon nanotubes with controlled nitrogen content and modulated structure, and may provide an insight in developing various nitrogen-doped carbon-based nanodevices.

© 2012 Elsevier B.V. All rights reserved.

1. Introduction

During the past decade carbon nanotubes (CNTs) have been extensively studied due to their outstanding electrical and mechanical properties [1–4]. Numerous applications have been developed by using CNTs as device components in sensors [5,6], fuel cells [7–10], field emission devices [11], transistors, logic circuits [12–14], and high performance energetic nanomaterials [15]. Nitrogen-doped carbon nanotubes (CNx) have attracted considerable attention due to the possibility to tailor and improve the physical properties of pure carbon nanotubes [16–18]. Depending on the size and chirality of the nanotubes, CNx are either metallic or narrow gap semiconductors. The presence of additional lone pairs of electrons facilitates the injection of the electrons into the conduction band [19]. Low concentration doping of nitrogen into CNTs would make it possible to enhance the electronic conductance and surface reactivity of the tubes without deteriorating the mechanical properties [20]. However, the correlation between the nitrogen doping, microstructure and electrical transport behaviors of the low nitrogen doped CNTs still needs to be carefully investigated. These factors are key points in the development of CNx-based functional components such as improved catalyst support materials in proton exchange membrane fuel cells and

durable composite materials. Various techniques have been used for CNx synthesis including arc discharge [21], ion implantation [22], and diverse techniques based on chemical vapor deposition (CVD) [23,24]. Among these techniques, spray pyrolysis CVD reveals promising results in CNT synthesis. It provides a controlled way of spraying complex carbonaceous liquids mixed with catalyst containing molecules (metallocene powders) directly into the deposition chamber and ensures semi-continuous growth of CNTs [25]. Spray pyrolysis experiments usually require high flow rates of carrier gas and display difficulties in obtaining catalyst free CNTs with uniform diameters [26]. When low flow rates of carrier gas were used, the reactant solution could not be sprayed and fully evaporated, leaving behind metallocene residues [27]. Previously, vertically aligned nitrogen-doped CNTs have been prepared by spray pyrolysis method, in which the influence of hydrogen, temperature, precursor type and feeding amount on the nitrogen incorporation, nanotube structure and properties has been separately addressed [28–30]. Nevertheless, reports still remain few in terms of correlating a relationship between nitrogen doping, structure and electrical transport properties of nitrogen-doped CNTs. In addition, practical applications of doped nanotubes necessitate a precise and controlled introduction of dopants and a fairly large amount of material preferably in aligned configuration.

In this work, vertically aligned CNTs with modulated nitrogen concentration were grown on semiconducting Si using a modified spray pyrolysis CVD method without hydrogen addition. Mixtures of ferrocene, xylene, and acetonitrile were directly sprayed over

* Corresponding author. Fax: +1 519 661 3020.

E-mail address: xsun@eng.uwo.ca (X. Sun).

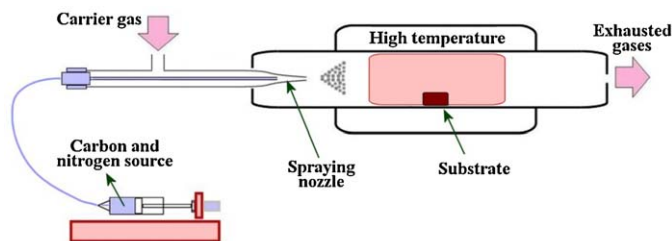


Fig. 1. Schematic illustration of spray pyrolysis CVD system for CN_x synthesis.

the substrate at a low flow rate of carrier gas (175 sccm) without affecting the spraying process or the evaporation of the catalyst. The correlation between the nitrogen doping concentration, nitrogen chemical environment, structure and crystallinity of the nanotubes was investigated and the dependence of the electrical transport properties of the nanotubes on the nitrogen content, temperature and pressure was also addressed.

2. Experimental

The CVD system used in this study consisted of an electronically controlled furnace with 300 mm effective heating length, a quartz reactor tube (i.d. 25.4 mm), and a spraying setup. The device developed for spraying liquids at low flow rates consisted of a carrier gas tube (i.d. 4.2 mm) which ended with a spraying nozzle (i.d. 0.5 mm) and a sealed inner tube (i.d. 1.5 mm) carrying the active solution. The pressure formed inside the carrier gas tube pulverized the solution even at low flow rates, through the nozzle, inside the deposition chamber, up to the substrate surface situated in the middle of the quartz tube. The deposition system and the injection device are presented in Fig. 1.

In this study, oriented n-type (1, 0, 0) silicon (Si) wafers were used as a substrate, without removing the native oxide layer. An aluminum (Al) under-layer, with the thickness of 30 nm, was magnetron sputtered on the Si substrate to effectively prevent the catalyst particles from aggregation. The active solution of 0.01 g/ml concentration was prepared by dissolving ferrocene (Fe(C₅H₅)₂) into mixture of xylene (C₆H₄(CH₃)₂) and acetonitrile (CH₃CN). Ferrocene was used to produce metallic iron particles and to act as catalyst during the synthesis process and the xylene:acetonitrile mixture produced the C:N feedstock. The solution was continuously sprayed into the quartz reactor when the temperature reached 750 °C. In the spraying process, argon was used as the carrier gas at a flow rate of 175 sccm. The reaction was maintained for 4 min to inject a total amount of 3 ml solution at a feed rate of 0.75 ml/min in the CVD system. After the growth, the reactor was allowed to cool down under argon flow before exposure to air. Samples were characterized by scanning electron microscopy (SEM – Hitachi S-4700), Raman spectroscopy (Raman – Renishaw 785 nm laser excitation), and transmission electron microscopy (TEM – Philips CM-10). The TEM samples were prepared by sonicating a small piece of as-grown nanotubes in ethanol for 10 min and drying a few drops of suspension on a Cu micro-grid. The nitrogen amount was determined by X-ray photoelectron spectroscopy (XPS – Kratos AXIS Ultra, AlK α). *I*-*V* characteristics of the nitrogen-doped nanotubes were measured following a two-point probe model. The measurement system contained a DC power supply (Agilent E3644A) and a digital multimeter (Agilent 34410A). The carbon nanotubes were collected from substrates and 3 mg of powder was confined between gold plated aluminum conductors (2.5 mm diameter) and pressed at 60 kPa. Using this method, it led to the manufacture of microprobes containing nanotubes from experiments with different acetonitrile concentration.

3. Results and discussion

The nitrogen doping effects have been systematically examined by changing the concentration of acetonitrile in xylene. Five sets of experiments were conducted for a range of acetonitrile:xylene volume ratios of 0:100, 25:75, 50:50, 75:25, and xylene free.

3.1. Structure and composition of CN_x

SEM observation revealed an overall carpet-like deposit, containing highly dense and vertically aligned CNT arrays, for all samples. Acetonitrile was used as the nitrogen feedstock having a crucial influence on the tube growth. The length of the tubes ranged from 133 μ m to 12 μ m depending on the acetonitrile concentration. The maximum average tube length was obtained when no acetonitrile was in the solution. For experiments with 25 vol% acetonitrile in xylene, the average tube length sharply decreased to 47 μ m. The average tube length continued to decrease to 33 μ m for 50 vol% acetonitrile in xylene down to a minimum of 12 μ m for experiments done by using acetonitrile only (Fig. 2a). These observations indicate that the introduction of nitrogen species slows the nanotube growth and are in concordance with previous theoretical and experimental results [31,32]. The theoretical calculation has shown that nitrogen saturates the tube edge at the growing end and would not be as stable deeper in the hexagonal lattice. Higher nitrogen content would make the nanotube edge easier to be nitrogen saturated and, which favors the defect formation and slows the tube growth rate. The SEM image of the nanotube array root shows that the catalyst remains on the substrate during the growth process (Fig. 2b).

These observations are consistent with all experiments and indicate that the tubes grow upwards following a base growth mechanism. Moreover, physicochemical properties of nitrogen-doped CNTs depend greatly on nitrogen concentration, crystallinity and nanotube size such as diameter and wall thickness. Hence, dependence of the nanotube structure on the introduced acetonitrile concentration has been investigated. Fig. 2c and d shows TEM images of a nanotube at the bottom and tip part, respectively, confirming the base growth mode that the nanotube growth followed. Further TEM analysis reveals more detailed structural characteristics of CN_x. TEM investigations indicate that the samples contain neglected amount of amorphous carbon or catalyst particles encapsulated in the inner core or attached upon the nanotube surface. The nanotubes present typical defects occurred in a CVD process regardless to the structure changes caused by the incorporation of nitrogen. The change of the nanotube structure is presented in Fig. 3 using representative TEM images and Raman spectra of samples produced at 0%, 50%, and 100% acetonitrile concentrations. The micrographs of nanotubes produced from sole xylene are typical ones for regular carbon nanotubes produced by spray pyrolysis [26] and exhibit relatively well defined graphitic shells parallel to the tube axis (Fig. 3a and b). From the plotted diameter distribution on the basis of TEM images, the average outer diameter of the tubes is 42 nm (Fig. 3c) and the wall thickness is around 20 nm. Raman spectrum (Fig. 3d) indicates a strong band around 1583 cm⁻¹, which is referred to as the G-band. The G-band corresponds to the optical phonon modes of E_{2g} symmetry in graphite and indicates the formation of well graphitized carbon nanotubes. The D-band at 1352 cm⁻¹ originates from defects that occur in the curved graphene layers and at the tube ends. For estimating the defect concentration in carbon nanotubes the intensity of D-band from the Raman spectrum is usually normalized to the intensity of G-band. The intensity ratio of the D-band relative to G-band (*I*_D/*I*_G) for regular CNTs is *I*_D/*I*_G = 0.41. The presence of acetonitrile in the precursor changed the inner structure of the nanotubes. The tubes produced from precursors containing 25 vol% (not shown)

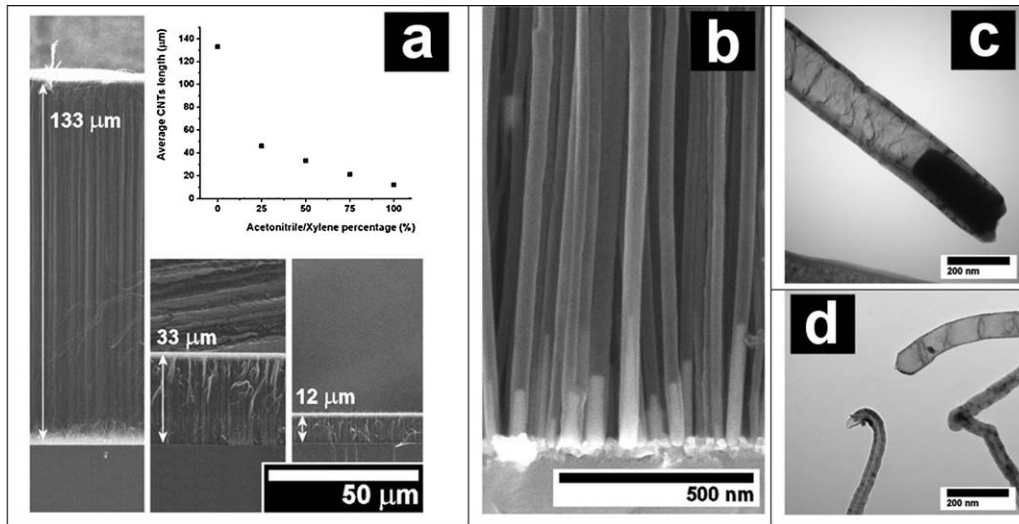


Fig. 2. Electron microscopic images showing average CNT length (a) (inset: diagram of the relationship between acetonitrile:xylene concentration and average CNT length) and nanotubes at the bottom (b and c) and tip part (d).

and 50 vol% acetonitrile become compartmentalized with lateral segmentation and exhibit stack-cone or bamboo structure (Fig. 3e and f).

The average outer diameter of the tubes increases to 51 nm (Fig. 3g) while the wall thickness slightly decreases to 16 nm. The Raman spectrum of the samples produced from precursor

containing 50:50 acetonitrile and xylene (Fig. 3h) shows an increase to 1.02 of the I_D/I_G ratio in comparison with the value $I_D/I_G = 0.41$ obtained for regular CNTs. The increase of I_D/I_G ratio for samples obtained from nitrogen containing precursors indicates that the tubes present lattice defects and disorders derived from nitrogen doping. The nanotubes produced from precursors containing

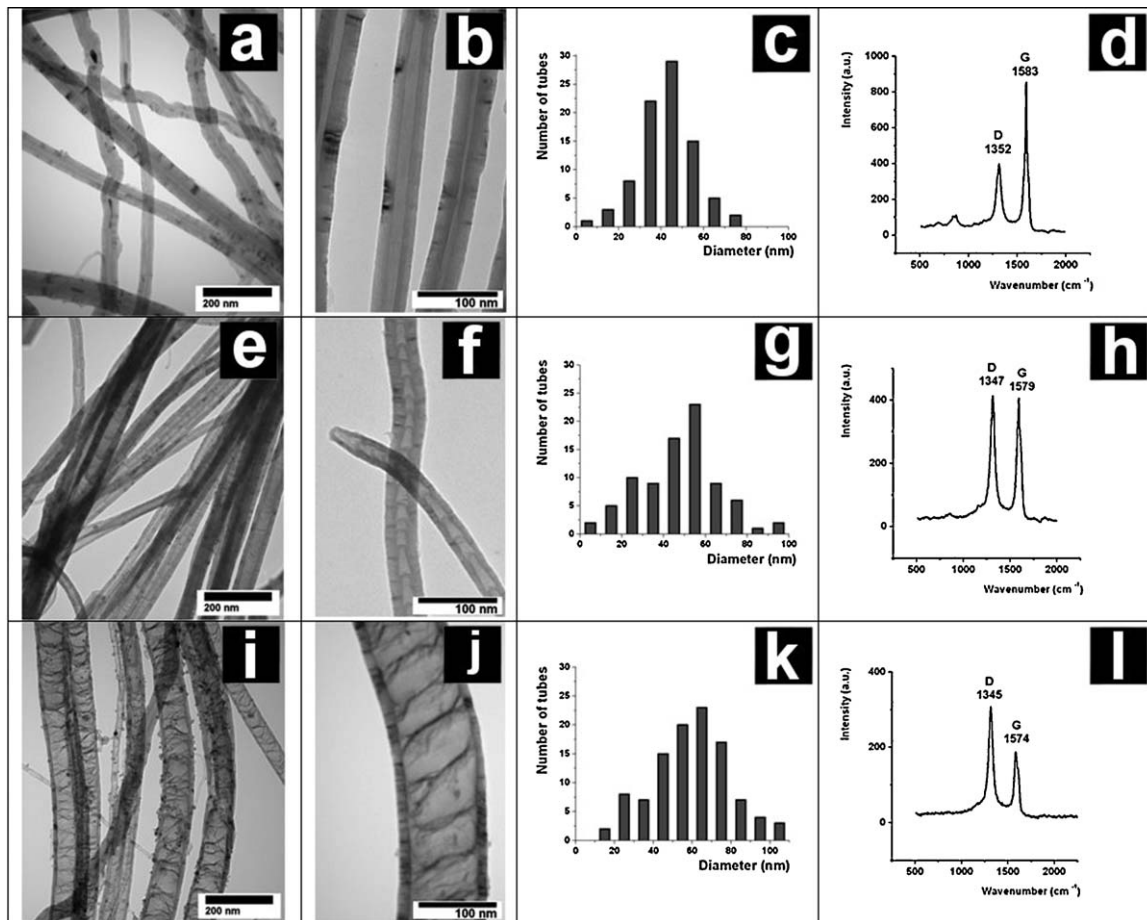


Fig. 3. TEM images of CNT structure, the diameter distribution, and the Raman spectrum for samples produced using pure xylene (a–d), 50 vol% concentration of acetonitrile in xylene (e–h), and pure acetonitrile (i–l).

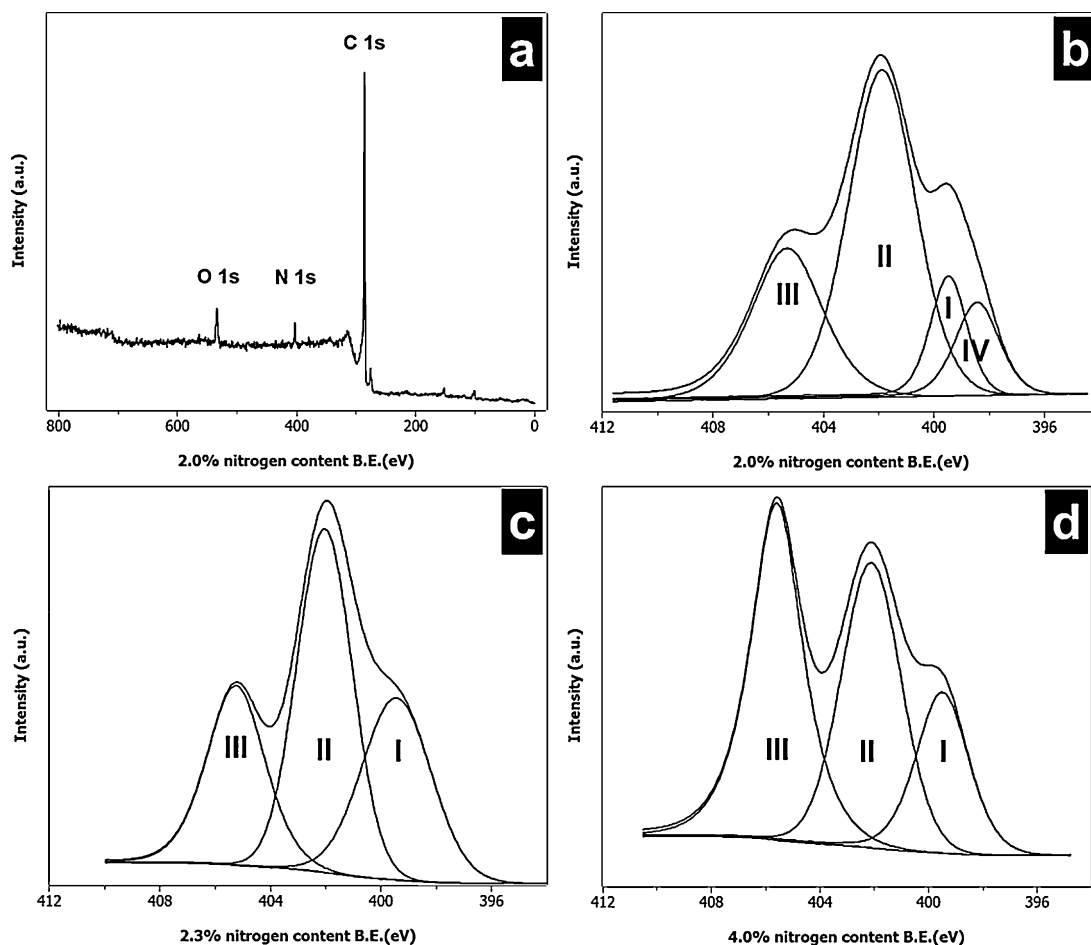


Fig. 4. A survey scan of the N-doped CNTs produced from 25 vol% acetonitrile (a) and N 1s XPS spectra of tubes produced from 25 vol% (b), 50 vol% acetonitrile (c), and from pure acetonitrile (d).

75 vol% acetonitrile (not shown) and from acetonitrile 100 vol% (Fig. 3i and j) present irregular and inter-linked corrugated structure. The average wall thickness of tubes decreases around 12 nm and the average outer diameter increases to 63 nm (Fig. 3k). These are reflected in a larger I_D/I_G ratio of 1.54 in the Raman spectrum (Fig. 3l). These observations indicate that the degree of long-range crystalline perfection of carbon nanotubes decreases with nitrogen presence in the synthesis process and are in agreement with previous reported observations resulted from pyrolysis of different nitrogen contained precursors such as melamine or benzylamine [24,32]. It can be observed that adding acetonitrile in the precursor mixture used for nanotube synthesis leads to a down-shift of the G-band from 1583 cm^{-1} (0% acetonitrile) to 1574 cm^{-1} (100% acetonitrile). Since the G-band is not related to the structural defects, the shift can be attributed to a modification in the electronic structure of the nitrogen doped tubes [33].

Based on the above analysis, it indicates that structure of the CNx can be modulated by changing acetonitrile concentration, in which nitrogen content within the nanotubes increases monotonously with increasing acetonitrile concentration, accordingly, crystallinity, diameter and wall thickness of nanotubes exhibit monotonous changes as well.

The correlation between the structure of nitrogen doped carbon nanotubes grown with various acetonitrile concentrations and incorporated nitrogen have been investigated by XPS measurements. The nitrogen doping concentration was determined from the atomic percentage ratio of nitrogen and carbon in the XPS measurements. Since the growth of CNTs was carried in Ar instead of N_2

flow, the nitrogen incorporation in the nanotube walls is a result of acetonitrile decomposition and is increased with the acetonitrile concentration in the feedstock. Adding 25 vol%, 50 vol%, and 75 vol% acetonitrile in the precursor resulted in doped nanotubes with 2 at.%, 2.3 at.%, and 3.6 at.% of nitrogen, respectively. Synthesis of nitrogen doped nanotubes from pure acetonitrile resulted in about 4 at.% nitrogen incorporation. Nitrogen can induce different configurations of bonding environments in the nanotubes assembly. Usually four types of nitrogen are found in CNx: pyridinic, graphitic, pyrrolic and molecular nitrogen [34–36]. The pyridinic nitrogen type is a nitrogen atom located at the edge or at a defect of the graphene sheet. The graphitic nitrogen is a nitrogen atom that substitutes a carbon atom located in the graphene sheet. Pyridinic and graphitic nitrogen are both sp^2 hybridized. The pyrrolic nitrogen is also substitutional, but is a part of a five-membered ring and is sp^3 hybridized. Molecular nitrogen can be encapsulated inside the tubes or exist as intercalated form between the graphite layers. Fig. 4a shows an XPS survey scan spectrum of the CNx prepared using 25 vol% acetonitrile. The peaks of C 1s, N 1s and O 1s are labeled at 285, 401 and 531 eV, respectively. The oxygen signal might originate from oxygen functional groups or the residual air in the nanotubes.

The N 1s XPS spectra of the nanotubes produced from 25 vol%, 50 vol% acetonitrile and from pure acetonitrile are presented in Fig. 4b–d. The N 1s peak can be deconvoluted into three main component peaks with binding energies of 398.6 eV (N1), 401.8 eV (N2), and 405.5 eV (N3). The low-energy N1 peak (I) at 398.6 eV is less intensive and corresponds to pyridine-like nitrogen. The peak

Table 1The structural changes of CN_x with different ratios of acetonitrile:xylene.

Acetonitrile:xylene	Nitrogen amount (at.%)	CNT wall structure	Average outer diameter and wall thickness (nm)	Average CNT length (μm)
0:100	–	Straight	42/20	133
25:75	2	Straight and bamboo	44/19	46
50:50	2.3	Bamboo and corrugated	51/16	33
75:25	3.6	Corrugated	56/15	21
100:0	4.0	Corrugated	63/12	12

N₂ (II) at 401.8 eV is more dominant and is attributed to graphitic nitrogen. The peak N₃ (III) at 405.5 eV is attributed to molecular nitrogen [13,37]. Molecular nitrogen is intercalated between the nanotube layers or encapsulated in the central nanotube hollow and thus it should have no influence on the structural characteristics of nanotubes [33]. In addition, a new peak at 397.8 eV (N₄) could be detected from the nanotubes in the case of using 25 vol% acetonitrile. The peak at 397.8 eV (IV) can be assigned to the tetrahedral nitrogen bonded to sp³-C probably due to un-decomposed N–H bond, which is similar to the case using octadecylamine as the precursor [37].

Furthermore, the ratio of pyridinic nitrogen to graphitic nitrogen increases with acetonitrile concentration from $I_{N1}/I_{N2} = 0.37$ (25 vol% acetonitrile) to 0.65 (50 vol% acetonitrile) and presents a maximum of 0.73 for pure acetonitrile. This suggests that the pyridine-like nitrogen doping increases with the acetonitrile concentration. The pyridine-like sites is considered to be responsible for the wall roughness and interlinked morphologies [38]. As the number of pyridinic nitrogen increases within the tubes, the roughness of tube walls and compartment layers also increases. These results are consistent with the TEM and Raman analyses and confirm that the defects and disorders of the tubes are dependent on the content of pyridinic nitrogen in the CNTs. The changes in tube morphology with the nitrogen concentration are summarized in Table 1.

3.2. Electrical resistivity of bulk CN_x

Bulk resistance of CN_x as ohmic *I*–*V* characteristics was measured following a two-point probe model. The measurements were conducted in the same oven used in the CVD process, at temperatures between 35 °C and 125 °C, monitored by a K type thermocouple. In order to achieve thermal equilibrium, the temperature of the system was kept for 10 min after the target temperature had been reached. For the temperature of 35 °C, all microprobes had almost the same electrical resistivity of $7.27 \times 10^{-3} \Omega \text{ m}$. With increasing temperature, the resistivity of the microprobes decreased monotonically. At the temperature of 85 °C, the resistivity of regular nanotubes produced from xylene was $7.10 \times 10^{-3} \Omega \text{ m}$ and that of the nanotubes produced using pure acetonitrile was $7.02 \times 10^{-3} \Omega \text{ m}$. At 125 °C, the resistivity of regular nanotubes was $6.96 \times 10^{-3} \Omega \text{ m}$, whereas that of the probe contained nanotubes obtained from pure acetonitrile was as low as $6.83 \times 10^{-3} \Omega \text{ m}$ (Fig. 5). These differences represent a change in resistivity of more than 29% between regular nanotubes and the tubes produced from pure acetonitrile indicating a better conductivity of CN_x. The temperature coefficient of resistance (TCR) gave the resistance change factor per degree of temperature change and was calculated from the formula $R = R_0[1 + \alpha(T - T_0)]$. The resulted TCR was $-4.7280 \times 10^{-4} \text{ K}^{-1}$ for regular nanotubes, decreased to $-5.7879 \times 10^{-4} \text{ K}^{-1}$ for nanotubes obtained from 50 vol% acetonitrile, and presented a minimum value of $-6.6915 \times 10^{-4} \text{ K}^{-1}$ for the nanotubes achieved using pure acetonitrile. The change of electrical resistance with pressure was measured following a similar procedure. The measurements were done at room temperature for the pressure interval of 40–139 kPa.

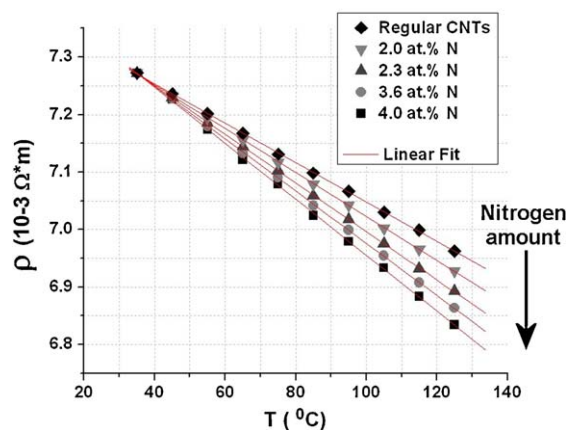


Fig. 5. The change of bulk CNT resistivity with temperature.

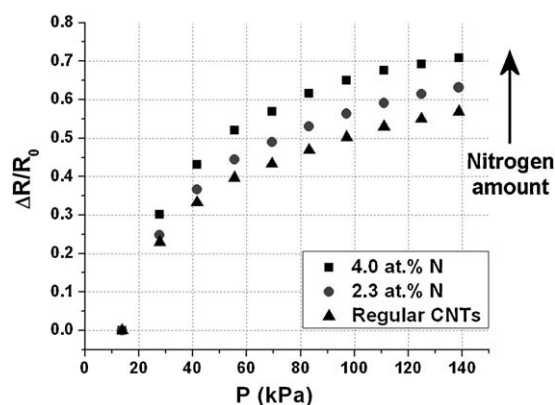


Fig. 6. The change of electrical resistance with pressure for bulk CNTs.

The change of electrical resistance increased with the nitrogen amount (Fig. 6) and the difference between regular nanotubes and the tubes produced from pure acetonitrile was about 20%. These measurements are in agreement with the results obtained by other groups [39–42], but could depend on sample preparation, material impurities, and the measuring conditions. It was indicated that the conduction occurs at the cross section of the nanotubes and is affected by inner structure of the tubes and by the applied compressive stress. While many factors influence the measurement results, this method is highly repeatable and a relatively simple tool to quantify the resistivity of bulk CNTs.

4. Conclusions

Vertically aligned CNTs with tuning nitrogen content have been synthesized on silicon wafers by a modified spray pyrolysis CVD method. The nitrogen concentration was tailored by changing the concentration ratio of nitrogen/carbon source during the spraying process. The incorporated nitrogen significantly influenced the tube structure from straight, bamboo to corrugated nanotubes, caused defects within the CN_x, and decreased the growth rate. The

ratio of pyridinic nitrogen to graphitic nitrogen in CNx increased with of acetonitrile/xylene ratio. Electrical measurements of the CNx with temperature and pressure indicate a better conductivity of bulk CNx as the nitrogen concentration inside the tubes increased. The present work introduces a versatile method of growing vertical aligned nitrogen-doped nanotubes and demonstrates that CNTs with modulated nitrogen, controlled structure, and controlled electrical transport properties can be obtained. It provides useful information in terms of both fundamental understandings and practical applications of CNx nanotubes in developing various CNx nanotube-based nanodevices and high performance energetic nanomaterials.

Acknowledgements

This research was supported by Department of National Defense (DND), Natural Sciences and Engineering Research Council of Canada (NSERC), Canada Research Chair (CRC) Program, Canada Foundation for Innovation (CFI), Ontario Research Fund (ORF), Ontario Early Researcher Award (ERA), Ontario Graduate Scholarship Program (OGS), and the University of Western Ontario.

References

- [1] P. Ajayan, Nanotubes from carbon, *Chem. Rev.* 99 (1999) 1787–1800.
- [2] R. Tenne, Inorganic nanotubes and fullerene-like nanoparticles, *Nat. Nanotechnol.* 1 (2006) 103–111.
- [3] J. Bernholc, D. Brenner, M.B. Nardelli, V. Meunier, C. Roland, Mechanical and electrical properties of nanotubes, *Annu. Rev. Mater. Sci.* 32 (2002) 347–375.
- [4] L. Qu, L. Dai, Gecko-foot-mimetic aligned single-walled carbon nanotube dry adhesives with unique electrical and thermal properties, *Adv. Mater.* 19 (2007) 3844–3849.
- [5] J. Kong, N. Franklin, C. Zhou, M. Chapline, S. Peng, K. Cho, H. Dai, Nanotube molecular wires as chemical sensors, *Science* 287 (2000) 622–625.
- [6] S. Ghosh, A. Sood, N. Kumar, Carbon nanotube flow sensors, *Science* 299 (2003) 1042–1044.
- [7] X. Sun, R. Li, D. Villers, J. Dodelet, S. Desilets, Composite electrodes made of Pt nanoparticles deposited on carbon nanotubes grown on fuel cell backings, *Chem. Phys. Lett.* 379 (2003) 99–104.
- [8] M.S. Saha, R. Li, X. Sun, S. Ye, 3-D composite electrodes for high performance PEM fuel cells composed of Pt supported on nitrogen-doped carbon nanotubes grown on carbon paper, *Electrochem. Commun.* 11 (2009) 438–441.
- [9] M.S. Saha, R. Li, X. Sun, High loading and monodispersed Pt nanoparticles on multiwalled carbon nanotubes for high performance proton exchange membrane fuel cells, *J. Power Sources* 177 (2008) 314–322.
- [10] Y. Chen, J. Wang, H. Liu, R. Li, X. Sun, S. Ye, S. Knights, Enhanced stability of Pt electrocatalysts by nitrogen doping in CNTs for PEM fuel cells, *Electrochem. Commun.* 11 (2009) 2071–2076.
- [11] S. Srivastava, V. Vankar, V. Kumar, Excellent field emission properties of short conical carbon nanotubes prepared by microwave plasma enhanced CVD process, *Nanoscale Res. Lett.* 3 (2008) 25–30.
- [12] T. Rueckes, K. Kim, E. Joselevich, G. Tseng, C. Cheung, C. Lieber, Carbon nanotube-based nonvolatile random access memory for molecular computing, *Science* 289 (2000) 94–97.
- [13] H. Postma, T. Teepen, Z. Yao, M. Grifoni, G. Dekker, Carbon nanotube single-electron transistors at room temperature, *Science* 293 (2001) 76–79.
- [14] A. Bachtold, P. Hadley, T. Nakanishi, C. Dekker, Logic circuits with carbon nanotube transistors, *Science* 294 (2001) 1317–1320.
- [15] Y. Zhong, M. Jaidann, Y. Zhang, G. Zhang, H. Liu, M.I. Ionescu, R. Li, X. Sun, H. Abou-Rachid, L. Lussier, Synthesis of high nitrogen doping of carbon nanotubes and modeling the stabilization of filled DAATO@CNTs (10,10) for nanoenergetic materials, *J. Phys. Chem. Solids* 71 (2010) 134–139.
- [16] M. Terrones, P. Ajayan, F. Banhart, X. Blase, D. Carroll, J. Charlier, R. Czerw, B. Foley, N. Grobert, R. Kamalakaran, P. Kohler-Redlich, M. Ruhle, T. Seeger, H. Terrones, N-doping and coalescence of carbon nanotubes: synthesis and electronic properties, *Appl. Phys. A: Mater.* A74 (2002) 355–361.
- [17] M. Terrones, A. Jorio, M. Endo, A. Rao, Y. Kim, T. Hayashi, H. Terrones, J. Charlier, G. Dresselhaus, M. Dresselhaus, New direction in nanotube science, *Mater. Today* 7 (2004) 30–45.
- [18] C. Ewels, M. Glerup, Nitrogen doping in carbon nanotubes, *J. Nanosci. Nanotechnol.* 5 (2005) 1345–1363.
- [19] Y. Huang, J. Gao, R. Liu, Structure and electronic properties of nitrogen-containing carbon nanotubes, *Synth. Met.* 113 (2000) 251–255.
- [20] R. Sen, B.C. Satishkumar, A. Govindaraj, K.R. Harikumar, G. Raina, J. Zhang, A.K. Cheetham, C.N.R. Rao, B-C-N, C-N and B-N nanotubes produced by the pyrolysis of precursor molecules over Co catalysts, *Chem. Phys. Lett.* 287 (1998) 671–676.
- [21] M. Glerup, J. Steinmetz, D. Samaille, O. Stephan, S. Enouz, A. Loiseau, S. Roth, P. Bernier, Synthesis of N-doped SWNT using the arc-discharge procedure, *Chem. Phys. Lett.* 387 (2004) 193–197.
- [22] J. Kotakoski, A. Krashennnikov, Y. Ma, A. Foster, K. Nordlund, R. Nieminen, B and N ion implantation into carbon nanotubes: insight from atomistic simulations, *Phys. Rev. B* 71 (2005), 205408–205408-6.
- [23] C. Tang, Y. Bando, D. Goldberg, F. Xu, Structure and nitrogen incorporation of carbon nanotubes synthesized by catalytic pyrolysis of dimethylformamide, *Carbon* 42 (2004) 2625–2633.
- [24] H. Liu, Y. Zhang, R. Li, X. Sun, S. Desilets, H. Abou-Rachid, M. Jaidann, L. Lussier, Structural and morphological control of aligned nitrogen-doped carbon nanotubes, *Carbon* 48 (2010) 1498–1507.
- [25] M.I. Ionescu, Y. Zhang, R. Li, X. Sun, H. Abou-Rachid, L.-S. Lussier, Hydrogen-free spray pyrolysis chemical vapor deposition method for the carbon nanotube growth: parametric studies, *Appl. Surf. Sci.* 257 (2010) 7837–7844.
- [26] L. Biró, Z. Horváth, A. Koós, Z. Osváth, Z. Vértsey, A. Darabont, K. Kertész, C. Neamtu, Z. Sárközi, L. Tapasztó, Direct synthesis of multi-walled and single-walled carbon nanotubes by spray-pyrolysis, *J. Optoelectron.* 5 (2003) 661–666.
- [27] C. Deck, G. Mckee, K. Vecchio, Synthesis optimization and characterization of multiwalled carbon nanotubes, *J. Electron. Mater.* 35 (2006) 211–223.
- [28] J. Liu, R. Czerw, D.L. Carroll, Large-scale synthesis of highly aligned nitrogen doped carbon nanotubes by injection chemical vapor deposition methods, *J. Mater. Res.* 20 (2005) 538–543.
- [29] M.S. He, S. Zhou, J. Zhang, Z.F. Liu, C. Robinson, CVD growth of N-doped carbon nanotubes on silicon substrates and its mechanism, *J. Phys. Chem. B* 109 (2005) 9275–9279.
- [30] T.X. Cui, R.T. Lv, Z.H. Huang, H.W. Zhu, J. Zhang, Z. Li, Y. Jia, F.Y. Kang, K.L. Wang, D.H. Wu, Synthesis of nitrogen-doped carbon thin films and their applications in solar cells, *Carbon* 49 (2011) 5022–5028.
- [31] B.G. Sumpter, V. Meunier, J.M. Romo-Herrera, E. Cruz-Silva, D.A. Cullen, H. Terrones, D.J. Smith, M. Terrones, Nitrogen-mediated carbon nanotube growth: diameter reduction, metallicity, bundle dispersability, and bamboo-like structure formation, *ACS Nano* 1 (2007) 369–375.
- [32] A. Koos, M. Dowling, K. Jurkschat, A. Crossley, N. Grobert, Effect of the experimental parameters on the structure of nitrogen-doped carbon nanotubes produced by aerosol chemical vapour deposition, *Carbon* 47 (2009) 30–37.
- [33] L. Bulusheva, A. Okotrub, I. Kinloch, I. Asanov, A. Kurenaya, A. Kudashov, X. Chen, H. Song, Effect of nitrogen doping on Raman spectra of multi-walled carbon nanotubes, *Phys. Status Solidi B* 245 (2008) 1971–1974.
- [34] P. Ayala, R. Arenal, M. Rummeli, A. Rubio, T. Pichler, The doping of carbon nanotubes with nitrogen and their potential applications, *Carbon* 48 (2010) 575–586.
- [35] P. Ayala, A. Grüneis, T. Gemming, D. Grimm, C. Kramberger, M.H. Rummeli, et al., Tailoring N-doped single and double wall carbon nanotubes from a nondiluted carbon/nitrogen feedstock, *J. Phys. Chem. C* 111 (2007) 2879–2884.
- [36] H.C. Choi, S.Y. Bae, W.S. Jang, J. Park, H.J. Song, H.J. Shin, et al., Release of N₂ from the carbon nanotubes via high-temperature annealing, *J. Phys. Chem. B* 109 (2005) 1683–1688.
- [37] K. Ghosh, M. Kumar, T. Maruyama, Y. Ando, Micro-structural, electron-spectroscopic and field-emission studies of carbon nitride nanotubes grown from cage-like and linear carbon sources, *Carbon* 47 (2009) 1565–1575.
- [38] H.C. Choi, J. Park, B. Kim, Distribution and structure of N atoms in multiwalled carbon nanotubes using variable-energy X-ray photoelectron spectroscopy, *J. Phys. Chem. B* 109 (2005) 4333–4340.
- [39] P. Singjai, S. Changsarn, S. Thongtem, Electrical resistivity of bulk multi-walled carbon nanotubes synthesized by an infusion chemical vapor deposition method, *Mater. Sci. Eng. A: Struct.* 443 (2007) 42–46.
- [40] L. Chen, C. Qin, X. Shi, S. Bai, L. Wang, High temperature electrical and thermal properties of the bulk carbon nanotube prepared by SPS, *Mater. Sci. Eng. A: Struct.* 420 (2006) 208–211.
- [41] R. Ma, C. Xu, B. Wei, J. Liang, D. Wu, D. Li, Electrical conductivity and field emission characteristics of hot-pressed sintered carbon nanotubes, *Mater. Res. Bull.* 34 (1999) 741–747.
- [42] Y.-H. Li, J. Wei, X. Zhang, C. Xu, D. Wu, L. Lu, B. Wei, Mechanical and electrical properties of carbon nanotube ribbons, *Chem. Phys. Lett.* 365 (2002) 95–100.